Geocarto International

ISSN: (Print) (Online) Journal homepage: https://www.tandfonline.com/loi/tgei20

Inversion of soil roughness for estimating soil moisture from time-series Sentinel-1 backscatter observations over Yanco sites

Ju Hyoung Lee & Jeffrey Walker

To cite this article: Ju Hyoung Lee & Jeffrey Walker (2020): Inversion of soil roughness for estimating soil moisture from time-series Sentinel-1 backscatter observations over Yanco sites, Geocarto International, DOI: 10.1080/10106049.2020.1805030

To link to this article: https://doi.org/10.1080/10106049.2020.1805030

GEOCARTO INTERNATIONAL
https://doi.org/10.1080/10106049.2020.1805030

Inversion of soil roughness for estimating soil moisture from time-series Sentinel-1 backscatter observations over Yanco sites

Ju Hyoung Lee[a] and Jeffrey Walker[b]

[a]Research Institute for Mega Construction, Korea University, Seoul, Republic of Korea; [b]Department of Civil Engineering, Monash University, Clayton, Australia

ABSTRACT
Sentinel-1 provides improved temporal and spatial resolutions in comparison with previous satellite missions. Unlike the change detection method that assumes the time-invariance of surface roughness at a coarse resolution, this study spatially inverted roughness and soil moisture from Sentinel-1 backscatter. Although it is important at high-resolution, local measurements of surface roughness are not available in an operational setting. Thus, question was how often time-varying soil roughness information should be updated in operations for reasonable soil moisture retrievals but at effective computational cost. Local validations show that a monthly update for surface roughness is sufficient for soil moisture retrievals. In more details, Root Mean Square Errors (RMSE) of 0.01 m^3/m^3 is found at Yanco A3 site, and 0.03 m^3/m^3 at Yanco A5 site, with differences in backscattering between Integral Equation Model (IEM) simulation and Sentinel-1 measurement of 0.78 dB at Yanco A3 site and 0.012 dB at Yanco A5 site, respectively.

ARTICLE HISTORY
Received 19 April 2020
Accepted 23 July 2020

KEYWORDS
Synthetic Aperture Radar (SAR) soil moisture; Sentinel-1; inversion of roughness; small-scale roughness

1. Introduction

Soil moisture is an important variable in the water, energy and carbon cycles. It is regularly used in hydrologic, land surface and climate model initialization, as it is fundamentally involved in the energy and water balance as a controlling factor on rainfall infiltration, energy flux, and deep drainage (Niu et al. 2011; Lee et al. 2014). The historical records of soil moisture accumulated over several years provide an essential indicator of climate change, while real-time soil moisture can be used for predicting urgent disasters such as landslides, flooding, and fire events (Henry et al. 2006; Jensen et al. 2018). However, despite significance, it is difficult to accurately simulate or predict soil moisture with models alone (Paloscia et al. 2013). That is because uncertainties arise from errors in rainfall, or soil hydraulic properties, and from the complex relationship between land surface state evolution and meteorological forcing (Taylor et al. 2012).

CONTACT Ju Hyoung Lee ju.lee@mail.com Research Institute for Mega Construction, Korea University, 145 Anam-ro, Seongbuk-gu, Seoul, Republic of Korea.
Supplemental data for this article can be accessed at https://doi.org/10.1080/10106049.2020.1805030.

One way to globally estimate the spatial distribution of soil moisture and simulate such a global circulation between land surface and meteorological forcing is to measure it with satellites. The microwave sensors that are predominantly used for estimating soil moisture operate at C- and L-bands. The first satellite that aimed for retrieving global soil moisture was the ESA (European Space Agency)'s Soil Moisture Ocean Salinity (SMOS) mission launched in 2009 (Kerr et al. 2012). The National Aeronautics and Space Administration (NASA)'s Soil Moisture Active Passive (SMAP) mission was the next soil moisture satellite launched in 2015. Both are passive microwave satellites operating at L-band (1.413 GHz, 21 cm, 2 to 3 day of revisit time). Their spatial resolutions are low at approximately 40 km, although their products are provided on the grids of 25 km or 9 km. The issue is that such low resolutions do not properly recognize the land surface heterogeneity (Kornelsen and Coulibaly 2013), which alter at the scale of meters.

In contrast, Sentinel-1, an active microwave sensor at C-band, provides high resolution data, although active microwave data are much more challenging to interpret. It is often discussed that difficulty arises from the radar signal complicated by dense vegetation or instrumental configuration. Sentinel-1A carries a Synthetic Aperture Radar (SAR) that operates at C-band (5.4 GHz) with dual polarization (VV + VH, HH + HV), and four exclusive acquisition modes of strip map, interferometric wide swath, extra-wide swath, and wave mode. Its incidence angle has a variation of $20 \sim 46°$ (Bauer-Marschallinger et al. 2019). Its revisit time is 12 days, while it is 3 days at equator.

Various approaches are available to retrieve soil moisture from SAR measurements (Kornelsen and Coulibaly 2013). Nonetheless, it still remains a complicated and ill-posed problem, because backscattering is not only affected by dielectric constant (i.e., soil moisture) but also by other variables such as soil roughness, volumetric scattering from the soil and vegetation, and SAR configuration including incidence angle, wavelength/frequency of instrument and polarization (Mirsoleimani et al. 2019). Moreover, soil moisture retrieval has the nature of equi-finality (Beven and Freer 2001). Multiple physical parameter combinations often produce the same SAR backscattering intensity. For example, wet soils produce a similarly high SAR backscatter intensity like rough soils, dense vegetation or rocks. Thus, for a successful retrieval, it is required to make an appropriate estimation of other physical parameters in order to isolate the contribution from soil moisture.

One of the common methods for retrieving soil moisture from active microwave sensors or scatterometers is change detection. It decomposes the radar backscattering into largely two simple elements: dielectric constant and roughness (Bauer-Marschallinger et al. 2019). In a dry state where the effects of dielectric constant are negated, it is considered that the radar backscattering comes from the surface roughness and vegetation only. In contrast, backscattering for wet soils is interpreted as soil moisture by subtracting backscattering in the dry conditions (i.e., roughness) . In other words, land surface homogeneity and time-invariance of surface parameters is assumed within low-resolution scatterometer footprint rather than estimating surface roughness or vegetation parameters. Thus, backscatter data at a coarse resolution and high temporal sampling have shown interesting results with this approach. However, such a change detection is not appropriate for high-resolution SAR data over spatially heterogeneous land undergoing vegetation distribution, tillage or soil erosion. Hence, with respect to the applicability of change detection, Wagner et al. (1999, 2010) clarified that to assume time-invariance of surface roughness is reasonable at low-resolution scatterometer, but inapplicable to high-resolution. Sentinel-1 SAR data corresponds to the latter.

One of the useful approaches to retrieve such heterogeneous land surface parameters at high-resolution is an inversion. Unlike change detection, it characterizes the physical parameters by minimizing the difference between model estimates and instrument measurements (Pauwels et al. 2002). This inversion approach is still useful, although other approaches such as fractal method or Artificial Neural Networks (ANNs) are suggested to estimate SAR roughness, recently. That's because they all require some roughness inputs as *a priori*. For example, to generate fractal surface, spatially distributed root-mean-square heights are needed. This SAR roughness is fundamentally different from roughness measured in the field, due to difference in scale and various instrumental factors to have an influence on backscatter. In addition, when estimating SAR roughness or soil moisture with ANNs, we still need to provide roughness inputs used as 'target' vectors (i.e., desired outcome). Thus, despite other alternatives, the need for inversion methods is very clear.

Several studies employed inversion methods for SAR retrievals. van der Velde et al. (2012) inverted soil roughness by comparing the ENVISAT Advanced Synthetic Aperture Radar (ASAR) backscattering measured from three different incidence angles with the IEM (Integral Equation Model) backscattering. They discussed that an enhanced temporal resolution is needed, suggesting to apply the approach for Sentinel-1 data as future works. Pierdicca et al. (2010) retrieved soil moisture content in a vegetated area, using multi-temporal Airborne SAR and biomass data from Landsat reflectance to correct the effects of vegetation. After generating a probability distribution function of a target parameter conditioned to SAR backscattering, soil moisture was inverted from backscattering. They concluded that this inversion approach better deals with ill-posed problems complicated by vegetation.

For supporting an inversion, Look Up Table (LUT) has also been widely used (Rahman et al. 2007; Merzouki et al. 2011). Forward model outputs of backscattering are established for a diverse range of input parameters, for example, soil roughness conditions, dielectric constant or incidence angle. The physical parameters to produce the similar backscattering coefficients with the backscattering measurements are selected from the LUT.

On the other hand, soil moisture can also be stochastically retrieved with a Bayesian approach, which uses the probability distribution function (PDF) generated by a broad range of dielectric constant and roughness conditions. This is a very useful method for resolving a perplexing retrieval problem of estimating soil roughness from SAR backscattering (Lee 2016). Verhoest et al. (2007) resolved uncertainty in soil roughness with a probabilistic approach for the estimation of soil moisture with the European Remote Sensing (ERS) scatterometer. After generating the PDFs of soil moisture with backscattering coefficients modeled with a possible range of Root Mean Square (RMS) height and correlation length, the mean value of the PDFs was used for determining optimal soil moisture values. RMS errors in soil moisture was less than 6%. Notarnicola et al. (2006) attempted to find the optimal soil moisture in a vegetated area by taking an average of PDFs. They assumed a Gaussian distribution for generating the PDFs of backscattering coefficient with an IEM simulation in various soil and vegetation water content conditions, and assessed the PDFs with soil parameter measurements. Synergy with optical data improved their parameterization of PDF shape.

In this study, we inverted time-varying soil roughness from backscattering to consider the dynamics of high-resolution land surface heterogeneity. The objective of this study is to retrieve low to medium levels of soil moisture in sparsely vegetated soils without relying on any soil parameter measurements in the field or multi-angular acquisitions, but with an inversion method applicable to small scale-roughness.

2. Methods

2.1. Study area

The Yanco site was established for the purpose of validating Soil Moisture Active Passive (SMAP) soil moisture data. It is a large flat area where barley and wheat are often grown. Two local stations at Yanco sites are used; Yanco-A3 station is (hereafter called YA3) and Yanco-A5 (hereafter, YA5). We have chosen these sites, as they are considered to have stable roughness during specified periods. The YA3 local point station is located at −34.73521 latitude, and 146.08197 longitude (elevation: 132 m) while local point station YA5 is located at −34.712858 latitude and 146.127712 longitude (elevation: 136 m). The spatial domains are set to include these local point stations: latitude of −34.7399 to −34.7320 and longitude of 146.0780 to 146.0829 for YA3, and latitude of −34.7150 to −34.7110 and longitude of 146.1260 to 146.1299 for YA5. This corresponds to 2,475 pixels (i.e., 45×55 in latitude × longitude) for the YA5 site, while it is 4,895 pixels (i.e., 89×55 in the same dimension) for the YA3 site. The spatial domain sizes do not include large-scale topography due to scale-dependency of roughness.

Soil texture for both sites has been found to be silty clay (conversation with Dr. Jason Beringer). During this experiment period, two sites were almost bare soils with no vegetation growth. In details, the time-average of Leaf Area Index (LAI) was 0.225 at the YA3 site, and 0.279 at the YA5 site, with respect to the maximum LAI value of 10. Soil moisture data was acquired from the OzNet data archive (http://www.oznet.org.au/) (Smith et al. 2012). It was measured with SDI-12 soil moisture probes every 20 minutes. In this study, the 2018 soil moisture data of the top 5 cm layer was collected from Day of Year (DoY) 25 to 145 at the YA3 site, and from DoY 1 to 145 in YA5 site are used. The soil has never been frozen in these sites. The time-average of soil temperature at YA3 site is 22 °C during experiment period, while it is 27 °C at YA5 site. Unfortunately, the measurements of surface roughness (e.g., RMS height or correlation length) or rainfall data are unavailable.

2.2. Sentinel-1 data

Time-series of SAR backscattering data at C-land (5.4 GHz) for the period of January to May 2018 were used in this study. High resolution Interferometric Wide (IW) swath mode at Level-1 Ground Range Detected (GRD) has a spatial resolution of 20×22 m, and a pixel spacing of 10×10 m. Revisit time was 12 days over the Yanco sites. Polarization is VV + VH. Pass direction is a descending orbit with similar incidence angles of $35 \sim 38°$ over the study area.

Following pre-processing procedure yielded gridded time-series SAR images stacked over the experiment site and period. Because the VV-polarized IW data in GRD format was already multi-looked and projected to ground range at a pixel spacing of 10 m (high resolution), radiometric and terrain correction (Range-Doppler Terrain Correction) were carried out with ESA's Sentinel Application Platform (SNAP)-python tool to mitigate geometric distortions in SAR data arising from topography or geometry, after calibrating it by Laur et al. (2004). After co-registration, multi-temporal speckle filtering was performed for the time-series data sets.

2.3. SAR retrieval process

In this section, an inversion for surface roughness and soil moisture is described. Simply, it minimizes a difference between the Sentinel-1 backscattering measurement and IEM forward model estimate. In other words, this algorithm retrieves the physical conditions (i.e., RMS height, correlation length, and dielectric constant) that IEM-modelled backscattering produces Sentinel-1 backscattering.

2.3.1. IEM backscattering model

The IEM is a standard model to simulate the single backscattering coefficient under the physical conditions defined by dielectric constant, surface roughness, and SAR configuration (Fung 1994). It is based upon an exponential relationship between backscattering coefficient and soil dielectric constant (Bindlish and Barros 2000). Its limitation is that the sensitivity of backscattering to soil moisture changes, depending on soils. In other words, it tends to be constant in wet soils, while it overestimates dry soils (Verhoest et al. 2007).

This IEM forward model computes the backscattering coefficients as follows (Ulaby et al. 1982; Shi et al. 1997):

$$\sigma^{o}_{pp} = \frac{k^2}{2}\exp(-2k_z^2 s^2)\sum_{n=1}^{\infty} s^{2n}|I^{n}_{\mathrm{pp}}|^2 \frac{\mathrm{W}^n(-2k_{\mathrm{X}},0)}{n!} \tag{1}$$

where subscript pp indicates the polarization, k is the wave number and S is the RMS height. In addition, $k_x = k\ \sin\theta$, $k_z = k\ \cos\theta$, where, θ is incidence angle. $I_{\mathrm{pp}}{}^{\mathrm{n}}$ is a function of the Fresnel reflection coefficient, relative permittivity and permeability of the surface (for a more detailed formula, see Chen et al. (1995); Shi et al. (1997)), and W^n is the Fourier transform for the n th power of the normalized surface correlation function.

As seen from Equation (1), soil roughness and dielectric constant information are required to estimate backscattering with the IEM, in addition to SAR configuration such as frequency or incidence angle. Such variables become dimensions of the LUT. In details, for the generation of LUT, RMS height ranged from 0.22 to 3.92 cm by an increment of 0.05 cm, while correlation length ranged from 0.2 to 11.2 cm by an increment of 0.1 cm. The Autocorrelation Function (ACF, the height probability distribution function of random surface) has been set as an exponential shape for relatively smooth surface (Davidson et al. 2000). The real part of the dielectric constant starts from 2.93 to 52.92 (Dobson et al. 1985; Reynolds et al. 2000; van der Velde et al. 2012).

2.3.2. Inversion of roughness

From the LUT generated in section 2.3.1, the retrieval algorithm selects soil roughness conditions (i.e., RMS height and correlation length) to minimize a difference in backscattering between IEM simulation and Sentinel-1 measurement, as follows:

$$\min\ |\sigma_{\mathrm{sentinel-1}} - \sigma_{\mathrm{IEM}}(\varepsilon,\ \mathrm{RH})| \tag{2}$$

where σ is backscattering, and subscript describes the source of backscattering. IEM backscattering is shown as a function of ε dielectric constant and RH soil roughness.

Roughness was updated approximately monthly, due to high computational cost. Soil roughness is assumed to be invariant during three Sentinel-1 measurement data acquisitions. This is a reasonable assumption, as the site remained as bare soils with no dramatic change in vegetation growth (see Supplementary Figure 1 for LAI) during the experimental period. In addition, relatively smooth surface roughness (e.g., kS less than 3) was assumed to ensure compliance with the IEM validity range (Mancini et al. 1999).

Table 1. Time-average soil moisture data.

	YA3	YA5
Average (m^3/m^3)	0.0372	0.1018
RMSE (m^3/m^3)	0.0103	0.030033
Bias (m^3/m^3)	−0.0009	−0.015691
Difference (dB)*	0.7808	0.012560

*difference is the difference between IEM and Sentinel-1 backscattering.

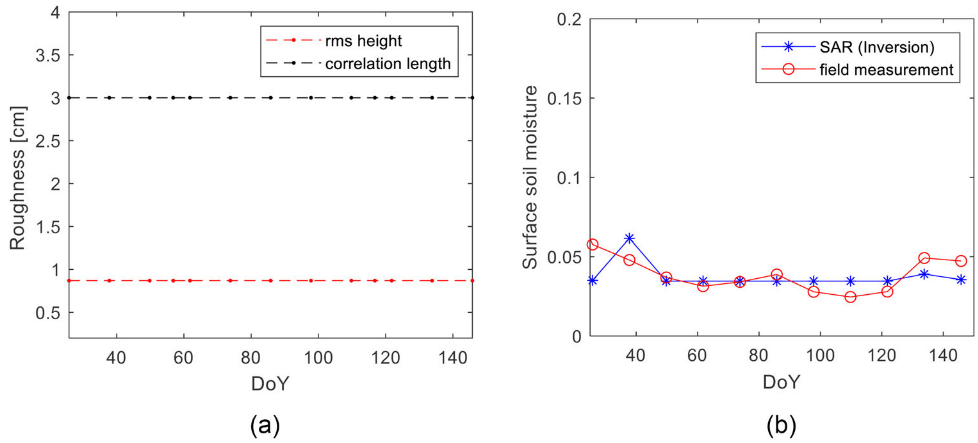

Figure 1. Surface conditions over YA3 site in 2018: (a) surface roughness (b) validation of SAR soil moisture

2.3.3. Estimation of soil moisture

With surface roughness estimated in section 2.3.2., soil moisture is retrieved. The dielectric constant value that yielded the smallest difference between IEM backscattering simulated for the roughness condition estimated in 2.3.2. and Sentinel-1 backscattering is selected, as follows:

$$\min \left|\sigma_{\text{sentinel}-1} - \sigma_{\text{IEM}}(\varepsilon)\right| \tag{3}$$

The limitation in this approach is that it assumes a stable surface condition. If the land surface changes over a short period of time, as in the agricultural season, a temporal sampling in the current data acquisition scheme may be too slow to appropriately retrieve the roughness.

3. Results and discussions

3.1. Local point validation for time-series SAR soil moisture

YA3 site is consistently dry at 0.049 m^3/m^3 on the time-average of soil moisture measured in the field during experimental period. SAR retrievals also report such soil dryness at 0.0372 m^3/m^3. Retrieval accuracy is considered satisfactory. As shown in Table 1, the Root Mean Square Error (RMSE) was found to be 0.01 m^3/m^3, showing a marginal difference between IEM simulated and Sentinel-1 measured backscattering coefficients at 0.78 dB. The dry bias was also very small at − 0.0009 m^3/m^3.

Time series soil moisture dynamics (top 5 cm) data for the YA3 site are presented in Figure 1. Some overestimation during DoY 100 to 120 is considered to be made because actual soils were drier than the minimum levels assumed in LUT. Overall, this retrieval algorithm appropriately estimates dry soils at YA3 site.

Unlike the YA3 site, time series soil moisture measurements were moderately wet in the YA5 site (see Figure 2). As shown in Table 1, the time-average of SAR soil moisture is also moderate at 0.1 m^3/m^3. RMSE was found to be 0.03 m^3/m^3, showing satisfactory results for the difference between IEM simulated and Sentinel-1 measured backscattering coefficients at 0.0126 dB. Negative biases were found being $-$ 0.016 m^3/m^3. It seems to be related to inversion errors in roughness (Lee 2016).

Based upon two different retrieval error structures discussed above, it is suggested that soil moisture retrieval errors are related to dependency on physical variables such as soil moisture

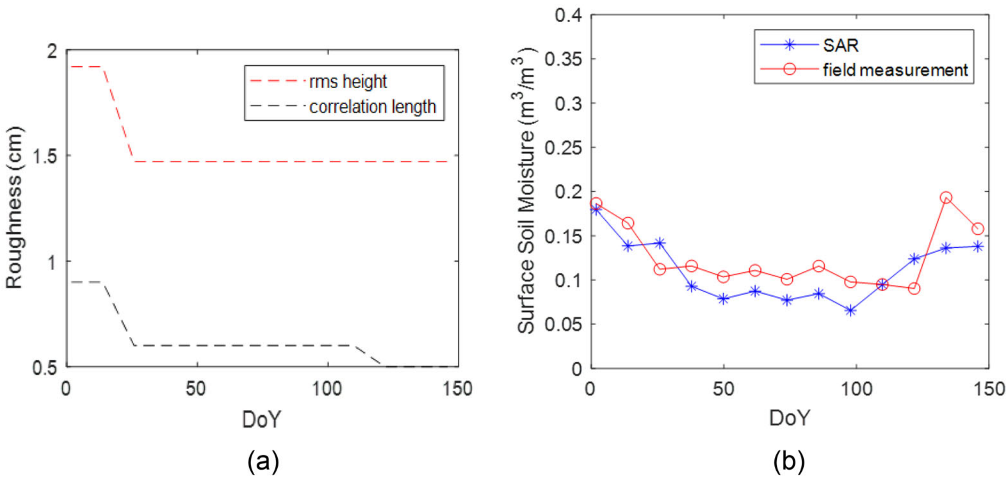

Figure 2. Surface conditions over YA5 site in 2018: (a) surface roughness (b) validation of SAR soil moisture.

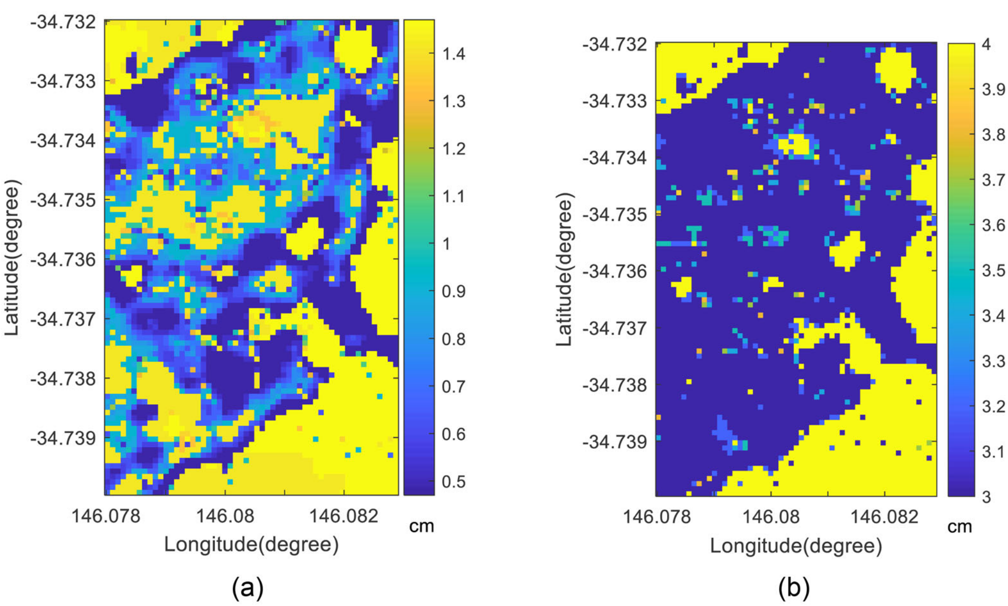

Figure 3. Surface roughness [cm] in YA3 site on DoY 60: (a) RMS height (b) correlation length.

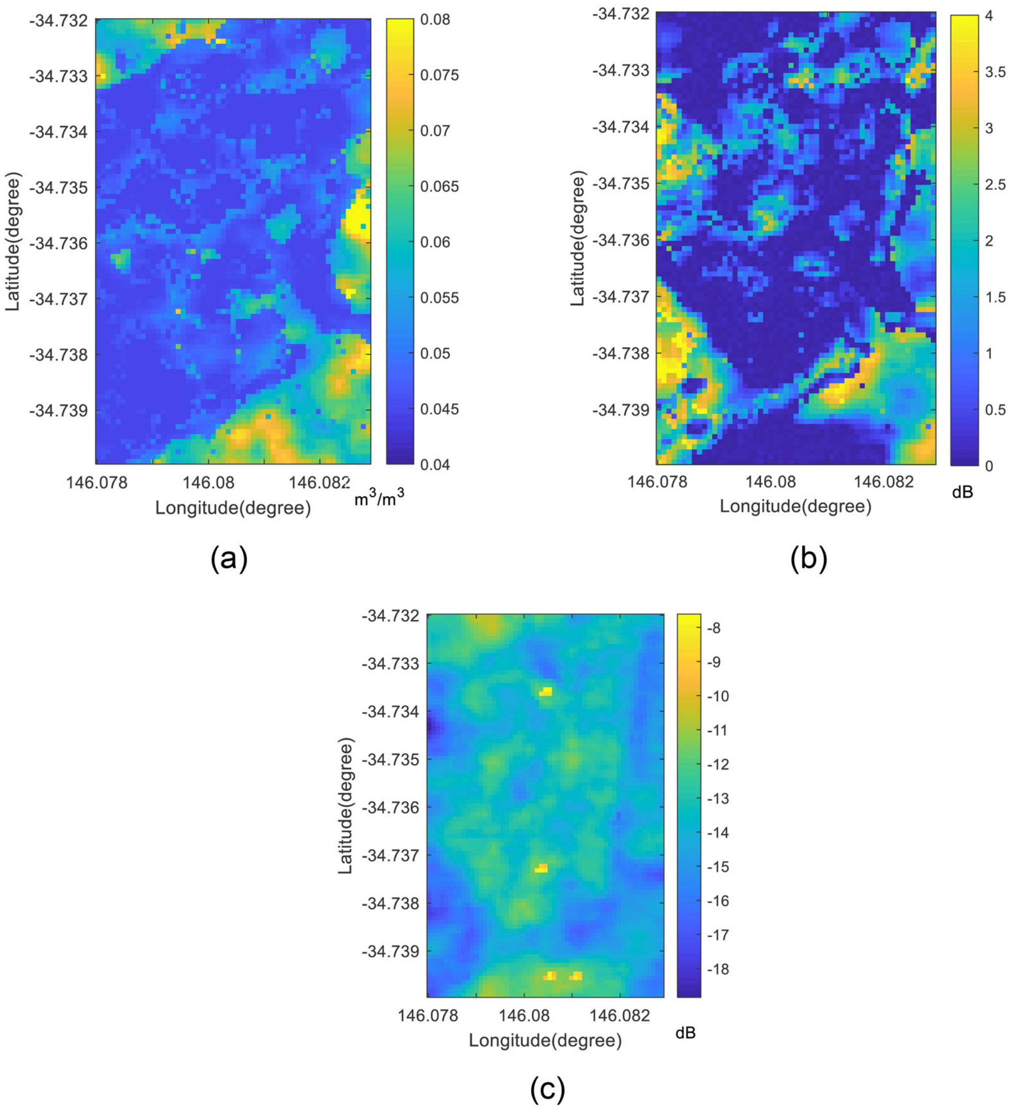

Figure 4. Spatial distribution for YA3 site on DoY 60: (a) soil moisture (b) difference in backscattering between IEM and Sentinel-1 and (c) Sentinel-1 backscattering. Units are indicated by color bars.

levels or surface roughness rather than season-dependent errors. However, this marginal level of retrieval errors seems acceptable, suggesting that a monthly update of roughness is reasonable under current surface conditions (i.e., LAI of $0.1 \sim 0.3$). Thus, it is stated that despite a sparse temporal sampling this retrieval method is appropriate when there is no weekly or daily change in vegetation growth or surface roughness. This is considered as the improvement of Sentinel-1 data, as compared to ENVISAT ASAR data (van der Velde et al. 2012).

3.2. Spatial distribution of SAR soil moisture

After validating the retrieval method over the local point measurement data, it is applied for estimating the spatial distribution of soil moisture.

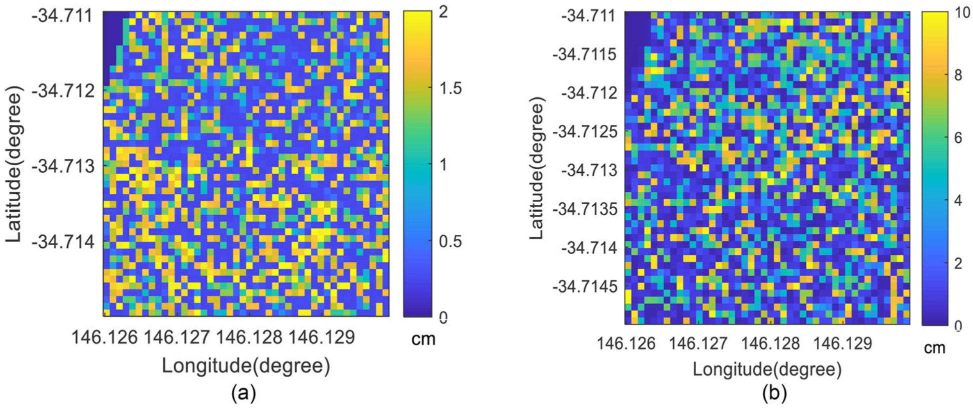

Figure 5. Surface roughness [cm] in YA5 site on DoY 121: (a) RMS height and (b) correlation length.

3.2.1. YA3 site

Figure 3 shows surface roughness over the area surrounding the YA3 site on DoY 60. In Figure 3(a), RMS height is shown to be spatially heterogeneous, ranging from 0.5 to 1.5 cm. The spatial average of RMS height was found to be 0.99 cm. In Figure 3(b), similarly to RMS height, the correlation length was also found to be spatially heterogeneous, ranging from 3.0 to 4.0 cm. The spatial average of correlation length was found to be 3.33 cm. The surface soil moisture retrieved with this roughness is further shown in Figure 4. In Figure 4(a), surface soil moisture was spatially mostly dry. The spatial average was 0.052 m^3/m^3.This is in agreement with the low soil moisture estimation of local field measurements shown in Figure 1.

It is thus stated that a spatial distribution of backscattering in YA3 site was related to roughness. More specifically, areas with high backscattering (shown yellow in Figure 4(c)) were closely related to RMS height in Figure 3(a) and low soil moisture in Figure 4(a). In other words, high backscattering is considered mostly due to roughness rather than soil moisture. The retrieval for these dry soils has a reasonable certainty, suggesting a difference between IEM simulated and Sentinel-1 measured backscattering was less than 0.89 dB. Thus, uncertainty is mostly low, as shown by dark blue in Figure 4(b). In contrast, other areas higher than 4 dB of backscattering difference (shown yellow in Figure 4(b)) suggest that a retrieval algorithm might underestimate (or overestimate) soil moisture there. As described in Section 2.3.1. and 3.1., error sources may be related to an assumption converting dielectric constant to soil moisture. It may be also affected by some ground features, or geometric errors in SAR (Zhu et al. 2019).

3.2.2. YA5 site

Figure 5 shows surface roughness over the YA5 site on DoY 121. Unlike the YA3 site, RMS height was spatially random, ranging from 0.52 to 2 cm in Figure 5(a). The spatial average of RMS height was found to be 0.796 cm. In Figure 5(b), similarly to RMS height, the correlation length was also random. The spatial average of correlation length was found to be 3.1 cm.

Surface soil moisture retrieved with this roughness condition is shown in Figure 6. In Figure 6(a), surface soil moisture was found to be moderately wet. Quantitatively, the spatial average of soil moisture was 0.1135 m^3/m^3. This level of soil moisture is similar to that found from local field measurements in Figure 2 and Table 1. Uncertainty for this estimation was

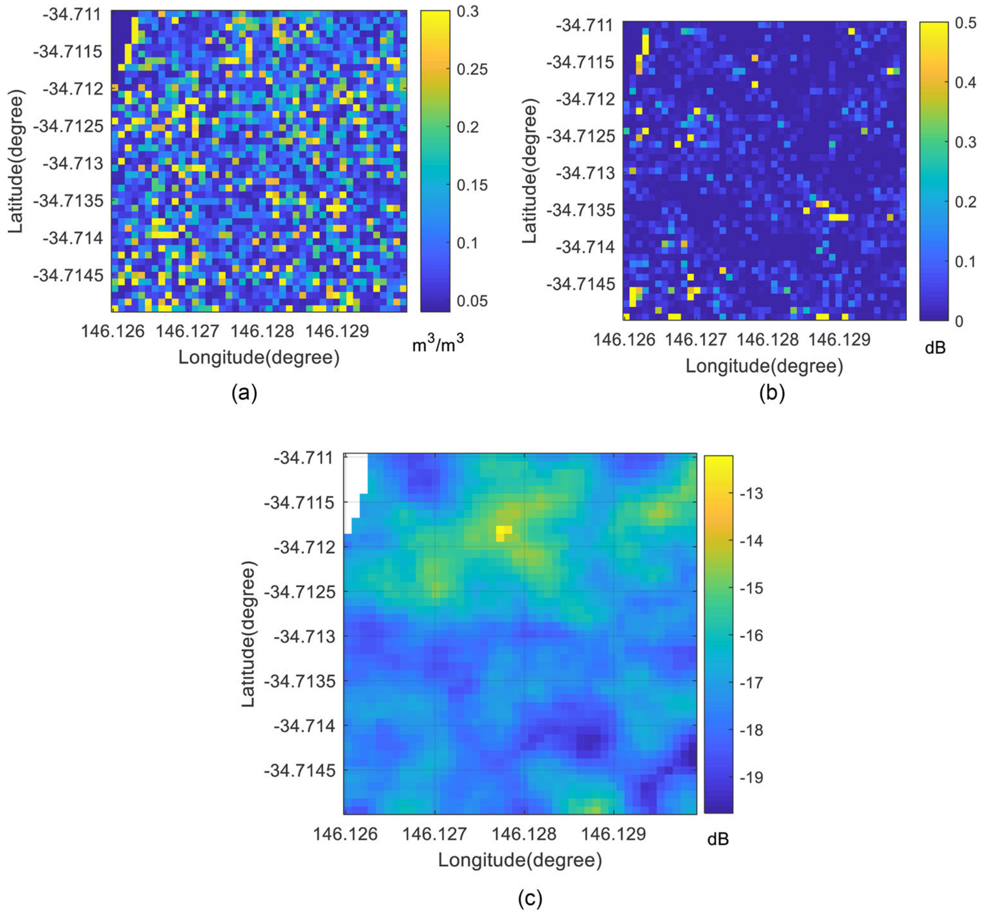

Figure 6. Spatial distribution in YA5 site on DoY 121: (a) soil moisture (b) difference in backscattering between IEM and Sentine-1 (c) original Sentinel-1 backscattering. Units are indicated by color bars.

also very little. The spatially averaged difference between the IEM simulated and Sentinel-1 measured backscattering was found to be very small at 0.024 dB in Figure 6(b).

It is suggested that the area with high backscattering (shown yellow in Figure 6(c)) was not directly related to soil moisture in Figure 6(a) or RMS height in Figure 5(a). Considering that overall uncertainty in retrieval is very low in Figure 6(b), it is stated that several factors other than soil moisture or roughness can elevate backscattering in a complicated way, and it is inappropriate to establish a direct and linear relationship between soil moisture and backscattering.

4. Conclusion

ENVISAT ASAR was the first SAR sensor that produces a global coverage over the land surface. However, for some operational reasons, a spatial coverage was irregular, and a temporal resolution was low. Thus, it was difficult to collect time-series data. Although ASCAT was operationally used for weather prediction models, its spatial resolution was still low. As compared to ASAR or ASCAT, Sentinel-1 data has improvements in terms of spatio-temporal resolutions. This study explored a retrieval algorithm to handle it in a computationally effective way.

For Sentinel-1 data, this study found that a monthly retrieval of surface roughness from time series Sentinel-1 backscattering measurements is sufficient for soil moisture retrievals, if surface condition is stable at LAI of 0.1 ~ 0.3. In detail, a high spatial variability of surface roughness at this small scale is appropriately expressed by this inversion approach, as spatial differences of backscattering between IEM simulated and Sentinel-1 were found to be small at 0.78 dB in YA3 site and 0.01 dB in YA5 site, respectively. the YA3 site in dry soils exhibited spatially patterned roughness, which was considered as the main contributor to backscattering variation. In contrast to the YA3 site, backscattering intensity in the YA5 site was found to have a more complicated relationship with soil moisture. Thus, it is suggested that this method fairly disentangled soil moisture from the backscattering effects of other physical parameters such as roughness, and high backscattering cannot be directly interpreted as wet soils. .

Due to assumption used for a retrieval of roughness, a change in vegetation conditions or surface roughness should be well-monitored during a retrieval of roughness with this algorithm. For example, a satellite-retrieved vegetation index should be associated with this retrieval in order to monitor any change in land surface. In addition, large scale topography would not be included for study domain. Thus, future works may suggest a strategy to invert roughness and soil moisture from SAR backscattering under the effect of volumetric scattering arising from time-varying vegetation. In addition, they will also investigate whether artificial neutral network can effectively estimate roughness despite this complicate and non-linear relationship between soil moisture and backscattering.

Disclosure statement

No potential conflict of interest was reported by the author(s).

Funding

This work was supported by the National Research Foundation of the Korean government (NRF-2018R1D1A1B07048817).

References

Bauer-Marschallinger B, Freeman V, Cao S, Paulik C, Schaufler S, Stachl T, Modanesi S, Massari C, Ciabatta L, Brocca L, et al. 2019. Toward global soil moisture monitoring with Sentinel-1: harnessing assets and overcoming obstacles. IEEE Trans Geosci Remote Sens. 57(1):520–539.

Beven K, Freer J. 2001. Equifinality, data assimilation, and uncertainty estimation in mechanistic modelling of complex environmental systems using the GLUE methodology. J Hydrol. 249(1–4):11–29. doi:.(01)00421-8

Bindlish R, Barros AP. 2000. Multifrequency soil moisture inversion from SAR measurements with the use of IEM. Remote Sens Environ. 71(1):67–88. doi:. (99)00065-6

Chen KS, Yen SK, Huang WP. 1995. A simple model for retrieving bare soil moisture from radar-scattering coefficients. Remote Sens Environ. 54(2):121–126. doi:. (95)00129-O

Davidson MWJ, Thuy Le T, Mattia F, Satalino G, Manninen T, Borgeaud M. 2000. On the characterization of agricultural soil roughness for radar remote sensing studies. IEEE Trans Geosci Remote Sens. 38(2):630–640.

Dobson MC, Ulaby FT, Hallikainen MT, El-Rayes MA. 1985. Microwave dielectric behavior of wet soil-Part II: dielectric mixing models. IEEE Trans Geosci Remote Sens. GE-23(1):35–46.

Fung AK. 1994. Microwave scattering and emission models and their applications. Norwood, MA: Artech House.

Henry JB, Chastanet P, Fellah K, Desnos YL. 2006. Envisat multi-polarized ASAR data for flood mapping. Int J Remote Sens. 27(10):1921–1929.
Jensen D, Reager JT, Zajic B, Rousseau N, Rodell M, Hinkley E. 2018. The sensitivity of US wildfire occurrence to pre-season soil moisture conditions across ecosystems. Environ Res Lett. 13(1):014021.
Kerr YH, Waldteufel P, Richaume P, Wigneron JP, Ferrazzoli P, Mahmoodi A, Al Bitar A, Cabot F, Gruhier C, Juglea SE, et al. 2012. The SMOS soil moisture retrieval algorithm. IEEE Trans Geosci Remote Sens. 50(5):1384–1403.
Kornelsen K, Coulibaly P. 2013. Advances in soil moisture retrieval from synthetic aperture radar and hydrological applications. J Hydrol. 476:460–489.
Laur H, Bally P, Meadows P, Sanchez J, Schaettler B, Lopinto E, Esteban D. 2004. Derivation of the backscattering coefficient in ESA ERS SAR PRI products. *ESA/ESRIN ES-TN-RS-PM-HL09*, 2: 1–55.
Lee HJ. 2016. Sequential ensembles tolerant to synthetic aperture radar (SAR) soil moisture retrieval errors. Geosciences. 6(2):19.
Lee JH, Pellarin T, Kerr YH. 2014. Inversion of soil hydraulic properties from the DEnKF analysis of SMOS soil moisture over West Africa. Agric for Meteorol. 188:76–88. doi:.
Mancini M, Hoeben R, Troch PA. 1999. Multifrequency radar observations of bare surface soil moisture content: A laboratory experiment. Water Resour Res. 35(6):1827–1838.
Merzouki A, McNairn H, Pacheco A. 2011. Mapping soil moisture using RADARSAT-2 data and local autocorrelation statistics. IEEE J Sel Top Appl Earth Obs Remote Sens. 4(1):128–137.
Mirsoleimani HR, Sahebi MR, Baghdadi N, El Hajj M. 2019. Bare soil surface moisture retrieval from Sentinel-1 SAR data based on the calibrated IEM and Dubois models using neural networks. Sensors. 19(14):3209.
Niu G-Y, Yang Z-L, Mitchell KE, Chen F, Ek MB, Barlage M, Kumar A, Manning K, Niyogi D, Rosero E, et al. 2011. The community Noah land surface model with multiparameterization options (Noah-MP): 1. Model description and evaluation with local-scale measurements. J Geophys Res. 116:D12109.doi:10.1029/2010JD015139.
Notarnicola C, Angiulli M., Posa F. 2006. Use of radar and optical remotely sensed data for soil moisture retrieval over vegetated areas. IEEE Trans Geosci Remote Sens. 44, 925–935.
Paloscia S, Pettinato S, Santi E, Notarnicola C, Pasolli L, Reppucci A. 2013. Soil moisture mapping using Sentinel-1 images: algorithm and preliminary validation. Remote Sens Environ. 134:234–248. doi:.
Pauwels VRN, Hoeben R, Verhoest NEC, De Troch FP, Troch PA. 2002. Improvement of TOPLATS-based discharge predictions through assimilation of ERS-based remotely sensed soil moisture values. Hydrol Process. 16(5):995–1013.
Pierdicca N, Pulvirenti L, Bignami C. 2010. Soil moisture estimation over vegetated terrains using multi-temporal remote sensing data. Remote Sens Environ. 114(2):440–448. doi:.
Rahman MM, Moran MS, Thoma DP, Bryant R, Sano EE, Holifield Collins CD, Skirvin S, Kershner C, Orr BJ. 2007. A derivation of roughness correlation length for parameterizing radar backscatter models. Int J Remote Sens. 28(18):3995–4012.
Reynolds CA, Jackson TJ, Rawls WJ. 2000. Estimating soil water-holding capacities by linking the Food and Agriculture Organization Soil map of the world with global pedon databases and continuous pedo-transfer functions. Water Resour Res. 36(12):3653–3662.
Shi JC, Wang J, Hsu AY, Neill PEO, Engman ET. 1997. Estimation of bare surface soil moisture and surface roughness parameter using L-band SAR image data. IEEE Trans Geosci Remote Sens. 35(5): 1254–1266.
Smith AB, Walker JP, Western AW, Young RI, Ellett KM, Pipunic RC, Grayson RB, Siriwardena L, Chiew FHS, Richter H. 2012. The Murrumbidgee soil moisture monitoring network data set. Water Resour Res. 48(7):W07701. doi:10.1029/2012WR011976.
Taylor CM, de Jeu RAM, Guichard F, Harris PP, Dorigo WA. 2012. Afternoon rain more likely over drier soils. Nature. 489(7416):423–426.
Ulaby F, Moore R, Fung A. 1982. Microwave remote sensing: Active and passive. In: Ulaby F, editor. Radar remote sensing and surface scattering and emission theory (Vol. 2). Norwood, MA: Artech House; p. 484–487.
van der Velde R, Su Z, van Oevelen P, Wen J, Ma Y, Salama MS. 2012. Soil moisture mapping over the central part of the Tibetan Plateau using a series of ASAR WS images. Remote Sens Environ. 120: 175–187.
Verhoest NEC, De Baets B, Mattia F, Satalino G, Lucau C, Defourny P. 2007. A possibilistic approach to soil moisture retrieval from ERS synthetic aperture radar backscattering under soil roughness uncertainty. Water Resour Res. 43(7):W07435. doi:10.1029/2006WR005295.

Wagner W, Noll J, Borgeaud M, Rott H. 1999. Monitoring soil moisture over the Canadian Prairies with the ERS scatterometer. IEEE Trans Geosci Remote Sens. 37(1):206–216.

Wagner W, Sabel D, Doubkova M, Bartsch A, Pathe C. 2010. The potential of Sentinel-1 for monitoring soil moisture with a high spatial resolution at global scale. In: Earth Observation and Water Cycle Science, Frascati, Italy, Volume: ESA SP-674, November 2010.

Zhu L, Walker JP, Ye N, Rüdiger C. 2019. Roughness and vegetation change detection: A pre-processing for soil moisture retrieval from multi-temporal SAR imagery. Remote Sens Environ. 225:93–106.